CHEMISTRY
A EUROPEAN JOURNAL

DOI: 10.1002/chem.200601514

Dipyrrolyl-Functionalized Bipyridine-Based Anion Receptors for Emission-Based Selective Detection of Dihydrogen Phosphate

Patrick Plitt, Dustin E. Gross, Vincent M. Lynch, and Jonathan L. Sessler*[a]

Abstract: New cationic anion receptors, based on the use of pyrrole-substituted bipyridine and coordinated to transition metals, are described. Specifically, polypyridine–ruthenium and –rhodium cores have been functionalized to generate an anion binding site. The design was chosen to probe the influence of the pyrrole-to-pyrrole separation on anion-binding affinities and selectivities; this distance is greater in the new systems of this report (receptors **1** and **2**) relative to that present in related dipyrrolyl quinoxaline based receptors **3** and **4**. Solution-phase anion-binding studies, carried out by means of ^{1}H NMR spectroscopic titrations in [D_6]DMSO and isothermal titration calorimetry (ITC) in DMSO, reveal that **1** and **2** bind most simple anions with substantially higher affinity than either **3** or **4**. In the case of chloride anion, structural studies, carried out by means of single-crystal X-ray diffraction analyses, are consistent with the solution-phase results and reveal that receptors **1** and **2** are both able to stabilize complexes with this halide anion in the solid state.

Keywords: anion receptors · hydrogen bonds · molecular recognition · pyrroles · sensors

Introduction

Synthetic anion receptor chemistry is one of the fastest growing disciplines in supramolecular chemistry.[1–12] Anions such as fluoride, chloride, and phosphate play critical roles in a range of biological processes and in the progression of a variety of diseases, ranging from fluorosis to cystic fibrosis.[13–15] Moreover, the nonspherical phosphate anion and more elaborate phosphorylated species play important roles in biochemical signaling, information processing, and energy storage.[16] While a number of naturally occurring anion receptors have been characterized in recent years, the de nova design of synthetic anion-binding agents remains a considerable challenge of tremendous current interest.[17] One approach that we, and others, have explored involves the use of pyrrole as the key anion-binding motif. Indeed, to date, a range of neutral and positively charged heterocyclic receptors comprising inter alia simple monomeric pyrroles, conjugated and nonconjugated open chain oligopyrroles, and various macrocyclic pyrrolic systems, have been described.[18] In the context of this work, it has been found that introduction of positive charges on the receptor by protonation or coordination of a metal cation generally enhances the binding affinity towards anions relative to the corresponding uncharged receptor system.[3,19] For instance, our group has introduced a new class of anion-binding agents based on dipyrrolyl quinoxalines (DPQ) and both our group and that of Anzenbacher have found that DPQ derivatives bearing coordinated transition-metal cations act as particularly effective anion-binding agents. An attractive feature of these latter systems is that they contain built-in chromophores (DPQ-derived backbone) and redox-sensing sites (metal centers).[20–23] In fact, the DPQ derivatives **3** and **4** have been found to interact particularly strongly with fluoride and allow for its selective naked-eye detection in DMSO.[24]

In light of these recent findings, we were interested in exploring whether the modification of the concave recognition cavity by elongation of the bridging site would lead to an enhanced affinity or to a variation in anion-binding selectivity such that the recognition of larger halide anions (i.e., chloride and bromide) or non-spherical oxoanions might be favored. Towards this end, we have now prepared the 4,4′-dipyrrolyl-2,2′-bipyridine (DPB)-based receptors **1** and **2**; compared to the earlier systems **3** and **4**, these new receptors permit the pyrrolic moieties, linked through the bipyridine spacer, to be separated by a greater distance. This criti-

[a] Dr. P. Plitt, D. E. Gross, Dr. V. M. Lynch, Prof. Dr. J. L. Sessler
Department of Chemistry and Biochemistry
The University of Texas at Austin, Austin, TX 78712 (USA)
Fax: (+1) 512-471-7550
E-mail: sessler@mail.utexas.edu

Supporting information for this article is available on the WWW under http://www.chemeurj.org/ or from the author.

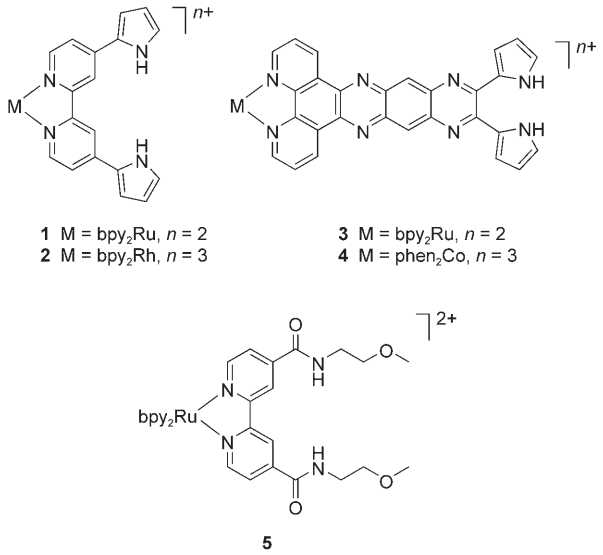

cal modification, which is inspired by the recent report of a ruthenium(II)-based bipyridine diamide receptor, **5**, by Beer and co-workers,[27] does indeed lead to enhanced affinity for relatively larger anions, in particular dihydrogen phosphate and benzoate at the expense of the smaller spherical halides (e.g., Cl^-).

Results and Discussion

The synthesis of metal complex-based receptors **1** and **2** is summarized in Scheme 1. Specifically, compound **6** was prepared in good yield by carrying out a Suzuki cross coupling between 4,4′-dibromobipyridine and *N*-Boc-protected pyrrole boronic acid in aqueous 1,2-dimethoxy ethane, followed by deprotection with sodium methoxide to give DPB (**7**). The ruthenium(II) and rhodium(III) complexes were obtained by reaction of the appropriate bis(2,2′-bipyridine) dichloro metal precursor with **7**. Chromatographic purification over silica gel using a acetonitrile/water/aqueous potassium nitrate solvent mixture as the eluent and subsequent treatment with an excess of ammonium hexafluorophosphate precipitated the complexes **1** and **2** from aqueous solution as their hexafluorophosphate salts in 33 and 79% yield, respectively (cf. Experimental Section).

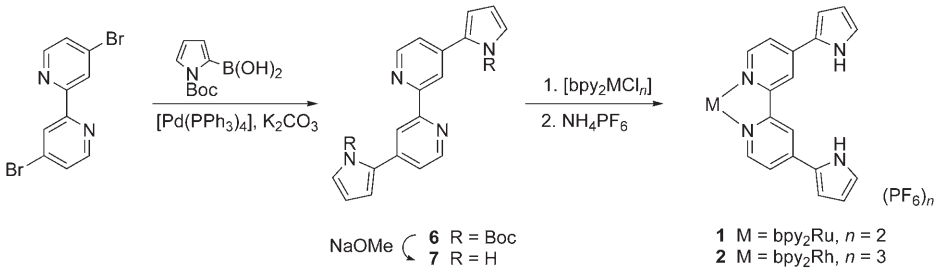

Scheme 1. Synthesis of the pyrrole substituted 2,2′-bipyridine complexes **1** and **2**.

The metal center present in receptors **1** and **2** provides a source of positive polarization that serves to withdraw electron density from the putative pyrrole-based binding site and should, therefore, enhance the interactions between the receptor and any appropriately sized negatively charged analyte. Metal complexation within the bipyridine subunit also serves to lock the conformation of the receptor into one that is expected to favor anion recognition on steric grounds. This combination of electronic effects, pre-organization, and larger pyrrole-based anion-binding cavity size (compared to the previously studied dipyrrolyl quinoxalines) was expected to lead to enhanced affinities for larger anions.

As a test of this hypothesis, the chloride, bromide, cyanide, benzoate, and dihydrogen phosphate anion-binding properties of receptors **1** and **2** were studied by UV/Vis, fluorescence, or ^{1}H NMR spectroscopy in DMSO or [D_6]DMSO, using the tetra-*n*-butylammonium (TBA) salt of the anion in question. The choice of this relatively competitive solvent was made so as to make more apparent any enhancements in anion binding affinity (if any) relative to what was seen in the case of receptors **3** and **4**. In this solvent, the formation of 1:1 host–guest complexes was inferred from so-called Job's plots in the case of F^-, Cl^-, Br^-, CN^-, $PhCO_2^-$, and $H_2PO_4^-$ and receptor **1** and in the case of Cl^-, Br^-, and $PhCO_2^-$ and receptor **2**. For chloride, bromide, cyanide, and benzoate, the anion-binding properties were explored by using ^{1}H NMR spectroscopic titration techniques. Figure 1, which is representative of the spectral

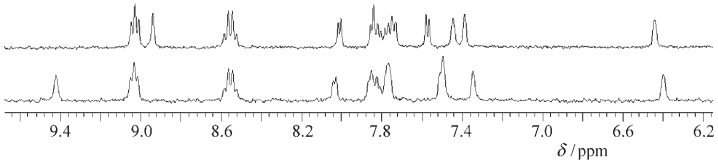

Figure 1. ^{1}H NMR spectrum (low-field region) of **2** in [D_6]DMSO (top) and in the presence of one equivalent tetrabutylammonium (TBA) chloride (bottom).

changes seen when anion binding occurs, illustrates the chemical shift changes recorded for receptor **2** upon the addition of increasing amounts of TBA-Cl. The largest concentration-dependent variation is observed for the inner CH proton *meta* to the pyridine nitrogen atom of the functionalized ligand.[25] These protons are well resolved over the entire range of the titration and are shifted downfield from $\delta =$ 8.8 to 9.6 ppm as a result of a direct interaction with the anion. Standard curve-fitting procedures were used to derive the corresponding affinity constants,[26] which, in accord with the proposed 1:1 binding interaction inferred from the corre-

sponding Job plot, were found to be concentration independent over the concentration range of 1.67 to 6.67 mM (1.67 to 3.33 mM for **1** and cyanide). The resulting K_a values are summarized in Table 1, along with those for the analogous ruthenium functionalized sensor **1** and the previously reported receptors **3**–**5**.[23,28]

Table 1. Association constants K_a [M^{-1}] for the interactions of receptors **1**–**5** with various anions in DMSO.[a]

	1[b]	**2**[b]	**3**[c,d]	**4**[c,d]	**5**[b,e]
F^-	7000±1600[c]	–[f]	12000	54000	–
Cl^-	370±50	870±50	10	20	150
Br^-	70±10	100±20	–	–	–
CN^-	500±80	–[f]	–	–	–
$PhCO_2^-$	2140±250	5090±510	–	–	–
$H_2PO_4^-$	104000±18000[g]	–[h]	40	50	1300

[a] Anions as TBA salts. [b] Determined by ^{1}H NMR spectroscopic titrations. [c] Based on UV/Vis spectroscopic titrations. [d] From reference [24]. [e] From reference [27]. [f] Nonspecific binding profile. [g] Determined by fluorescence spectroscopy. [h] Precipitation occurred during ^{1}H NMR titration.

Inspection of Table 1 provides support for the proposal that elongation of the spacing moiety can indeed be used to tune size recognition. For instance, while the DPQ-based receptors **3** and **4** bind chloride with a rather low affinity, DPB-derived complexes **1** and **2** display a chloride anion affinity that is about 40 times higher than their equivalently charged congeners. In agreement with the effect of charge seen in the case of systems **3** and **4**, the rhodium(III) receptor **2** binds chloride anion roughly twice as a well as its ruthenium(II) analogue **1**. The incrementally increased overall charge, from 2+ to 3+ upon going from **1** to **2**, also enhances the anion affinity for the two other anions that it proved possible to study with both receptor systems, namely bromide (small relative effect on the K_a value) and benzoate (K_a reduced by a factor of ca. 2; cf. Table 1). A comparison of **1** with the analogous ruthenium(II)-based bipyridine diamide receptor **5** reported by Beer and co-workers[27] shows that **1** binds chloride roughly 2.5 times as well in DMSO. This increase in affinity displayed by the newer pyrrole-containing ruthenium(II) bipyridine system **1** relative to **5** presumably reflects the fact that the highly flexible 2-methoxyethyl amide side chain present in Beer's system serves to preclude formation of a well organized binding site.

Whereas receptor **1** was found to bind cyanide anion cleanly and reversibly, in the case of complex **2**, additional peaks were seen in the ^{1}H NMR spectrum of receptor **2** upon the addition of approximately five equivalents of TBA-CN; the appearance of these new peaks was accompanied by a dramatic visual change from bright yellow to dark red. Analysis of the spectrometric changes by UV/Vis spectroscopy revealed the presence of a broad band at 520 nm, the intensity of which increased as the cyanide concentration was increased (see Supporting Information). The original yellow color of receptor **2** could be restored by the addition of water, which would implicate a pyrrole-centered deprotonation process.[28–31] In any event, the combined spectroscopic findings rule out a simple binding process involving only hydrogen bonding between cyanide and **2**, as appears to be operative in the case of **1**.

The divergent behavior of receptors **1** and **2** seen in the presence of cyanide emerged as even more apparent when TBA fluoride was titrated into solutions of **1** or **2** in DMSO. In the case of **1**, the formation of 1:1 host–guest complexes was inferred by ^{1}H NMR Job plot analysis and the observation of isosbestic points (at 386, 448, and 489 nm) during standard UV/Vis spectroscopic titrations. Identical affinity constants ($K_a = 7000 \pm 1600\ M^{-1}$) for the system **1**-$F^-$ were derived from both the ^{1}H NMR and UV/Vis spectroscopic titrations. In contrast, when F^- was added to receptor **2**, both the ^{1}H NMR nor UV/Vis spectroscopic titrations gave rise to binding profiles that could not be fit cleanly to a 1:1 binding process. Moreover, as observed in the case of CN^- a color change from yellow to red was seen in the case of F^- and **2**.

To explore the possible origin of this color change, tentatively assigned to a pyrrole-based deprotonation event, the non-nucleophilic base 1,8-diazabicyclo[5.4.0]undec-7-en was added to a solution of **2** in DMSO; this addition, as well as the separate addition of $LiN(SiMe_3)_2$, produced an immediate change from yellow to red. On this basis, we propose that the observed color change is due to deprotonation of receptor **2**, which—bearing a higher net charge—is expected to be more acidic than receptor **1**. This effect is seen to an appreciable extent only in the case of the relatively basic fluoride and cyanide anions, which, presumably, are able to deprotonate **2** in organic media, meaning that the formation of a hydrogen-bond-stabilized receptor–anion complex, to the extent it is produced, would only be expected in the case of such substrate–receptor pairs only at stoichiometric or substoichiometric guest-to-host ratios.

Unusual behavior was also seen when initial efforts were made to study the binding of dihydrogen phosphate by ^{1}H NMR spectroscopy. In fact, efforts at carrying out standard titrations were completely stymied by the fact that addition of TBA-H_2PO_4 to millimolar solutions of either **1** or **2** in [D_6]DMSO led to precipitation of the dihydrogen phosphate salt, as evidenced by ^{31}P NMR spectroscopic analysis. On the other hand, the fact that precipitation occurred led us to infer that the interaction between these two receptors and dihydrogen phosphate anion is appreciable. In other words, we expected to see a high affinity if conditions could be found in which the binding was reversible. This led us to explore the use of fluorescence spectroscopy, since the measurements in question could be carried out at a far lower concentration (ca. 1 μM vs. ca. 1 mM).

Sensor **1**, like other ruthenium(II) complexes, displays a red–orange emission, with irradiation of **1** at 464 nm giving rise specifically to an emission band with a maximum at 630 nm. No change in this band was seen when up to five molar equivalents of chloride, bromide, benzoate, hydrogen sulfate, and nitrate (all studied as the corresponding tetrabutylammonium salts) were added to a 1 μM solution of **1** in

DMSO at 25 °C. However, upon the stepwise addition of dihydrogen phosphate, the emission band at 630 nm gradually decreased (Figure 2). Aggregation of the host complex **1**

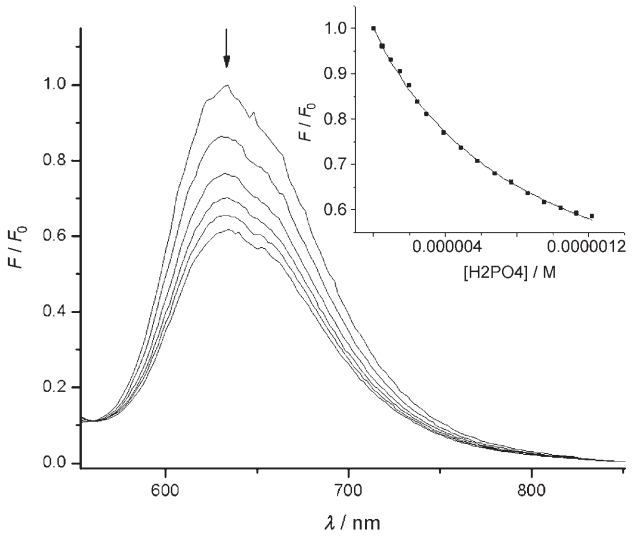

Figure 2. Fluorescence spectral changes of **1** (1 μM in DMSO) observed upon the addition of 0–9.5 equivalents of dihydrogen phosphate (TBA salt) at 22 °C. The inset shows a plot of F/F_0 versus $[H_2PO_4^-]$ at 630 nm.

could be ruled out on the basis of the linear Lambert–Beer behavior observed when the concentration range of the host **1** was varied between 0.05 and 50.0 μM. Accordingly, the changes in fluorescence intensity were ascribed to dihydrogen phosphate anion binding. Standard Job plot analysis revealed a 1:1 host to dihydrogen phosphate stoichiometry, as was seen in the case of the other anions under the more concentrated conditions of the ^{1}H NMR spectroscopic analyses. With this stochiometry established, plots of the relative fluorescence intensity (F/F_0) at a host concentration of 1.0 μM versus the guest concentration were used to determine the binding constant for the interaction between dihydrogen phosphate and host complex **1**. The resulting K_a value, 104 000 M^{-1}, is included in Table 1. This K_a value is approximately 2600-fold greater that the corresponding dihydrogen phosphate binding constant determined for the ruthenium(II)–DPQ derivative **3** and 80 times higher than that for the bipyridine diamide receptor **5**. It is worth noting that the minimal spectral changes observed in a control experiment involving the pyrrole-free parent tris(2,2′-bipyridine) ruthenium(II) complex could not be fit to any reasonable binding isotherm. This latter observation, coupled with the fact that shifts in the pyrrole NH signals are seen when the interactions with other anions are monitored by ^{1}H NMR spectroscopy, leads us to propose that receptors **1** and **2** bind anions through the dipyrrolyl binding site of the DPB ligand by specific hydrogen-bonding interactions, rather than by means of a nonspecific anion–cation associations.

In addition to ^{1}H NMR spectroscopic titrations, isothermal titration calorimetry (ITC) analyses were carried out to confirm the association constants for receptors **1** and **2** in the case of Cl^- and $PhCO_2^-$. ITC was chosen as a complementary method of study, since the required range of concentration overlaps with those used for the ^{1}H NMR spectroscopic titrations. In contrast to NMR spectroscopic methods, ITC analyses allows one to study the change in the heat of the whole system. It thus provides direct access to the energetics of the binding event without retreat to a structural probe (e.g., an NMR spectroscopic signal) that may or may not reflect the entirety of the associative process. Recently, in collaboration with Gale and Schmidtchen, we demonstrated that NMR spectroscopic titrations and ITC analyses give rise to concordant affinity constants when the conditions for the measurements are comparable.[32]

This conclusion, which was derived from an analysis of chloride anion binding to calix[4]pyrrole (**8**), is reinforced by the present study. In particular, a clean fit of the ITC data to a 1:1 stoichiometry model was observed ($N = 0.9$–1.0) when the titrations were carried out at a concentration range of the host between 0.9–2.9 mM in DMSO, a conclusion that is in agreement with the Job plot analyses in the case of the NMR studies (vide supra). As shown in Table 2, good agreement is seen for the affinity constants K_a obtained using these two disparate methods. For instance, the K_a for the interaction of chloride and **1** determined by NMR is (370 ± 50) M^{-1}, while the corresponding value resulting from ITC is 410 M^{-1}. Similar good agreement was seen in the case of **2**.

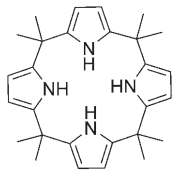

8

As observed previously for calix[4]pyrrole,[32,33] the formation of the present receptor–anion complexes in DMSO is largely driven by entropy. In the case of chloride, approximately 90% of the total energy ascribable to the binding is due to entropic factors. Based on this observation, we suggest that DMSO molecules are associated strongly to the free host compounds and that upon addition of chloride the free host is desolvated (enthalpically unfavored, $\Delta H > 0$) re-

Table 2. Selected thermodynamic data derived from isothermal titration calorimetry (ITC) for the interactions of receptors **1** and **2** with chloride and benzoate anions and comparison of the association constants K_a obtained by ^{1}H NMR titrations.[a]

	Anion	ΔG [kcal mol^{-1}]	ΔH [kcal mol^{-1}]	$T\Delta S$ [kcal mol^{-1}]	K_a [M^{-1}] (ITC)	K_a [M^{-1}] (NMR)
1	Cl^-	−3.56	0.41	3.96	410	370
1	$PhCO_2^-$	−4.35	−1.60	2.75	1560	2140
2	Cl^-	−4.13	0.49	4.62	1070	870
2	$PhCO_2^-$	−4.97	−1.03	3.93	4480	5090

[a] Anions were used as their TBA salts; the titrations were performed in DMSO; [host] = 2.9 mM (ITC) and 3.3 mM (NMR spectroscopy). Analyses were carried out at 25 and 22 °C, in the case of the ITC- and NMR-based studies, respectively.

leasing solvent molecules (entropically favored, $T\Delta S > 0$), which we propose provides a major driving force for the overall binding process. In the case of benzoate anion, about 65–80% of the total energy associated with binding to receptors **1** and **2** is ascribable to entropic factors. Interestingly, the enthalpy ΔH differs for the association of either **1** or **2** with chloride versus benzoate. Whereas ΔH is negative in the case of benzoate, the value is positive for chloride; this has the consequence that a correspondingly more favorable entropic term is required to give rise to an overall negative free energy, $\Delta G < 0$.

Further support for a pyrrole-NH–anion interaction came from single-crystal X-ray diffraction analyses of compounds **1** and **2** obtained in the presence of tetra-*n*-butylammonium chloride. The resulting structure for **1** reveals the anion lying in the plane defined by the four heterocyclic rings of the modified ligand and filling the concave cavity (Figure 3).

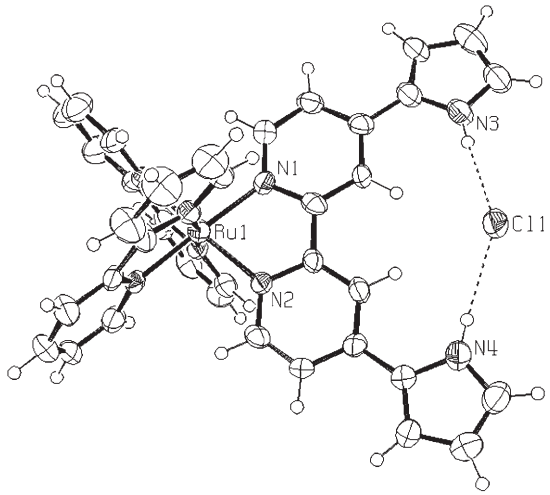

Figure 3. Structure of **1**·Cl with key atoms labeled shown looking down at the pseudo plane defined by the functionalized bipyridine subunit. The hexafluorophosphate anions and solvent molecules have been omitted for clarity. The thermal ellipsoids are scaled to the 50% probability level.

The chloride anion is hydrogen bonded to both pyrrolic moieties with N···Cl distances of 3.331(7) and 3.367(6) Å, respectively. Additionally, short atomic contacts (average C···Cl 3.65 Å) between pyridine CH protons and chloride are observed. The structure of **2** (Figure 4) is similar, but features slightly shorter N···Cl (3.306(4) and 3.312(4) Å) and C···Cl (3.59 Å) distances; presumably, this reflects the higher net charge of the metal complex and a correspondingly decreased electron density at the pyrrolic binding site.

In agreement with the solid-state structures reported previously for 2,2′-bipyridines, ligand **7** adopts a conformation in the crystal lattice that is *transoid* around the C–C bond connecting the two pyridine moieties (cf. Figure 5). The bond lengths and angles compare well to analogous pyrrolylpyridines.[34]

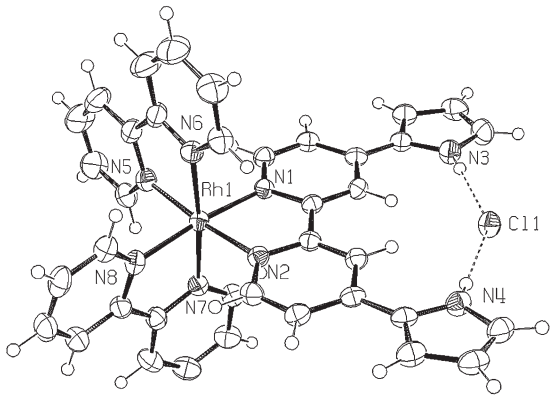

Figure 4. Structure of **2**·Cl with key atoms labeled. The hexafluorophosphate anions and solvent molecules have been omitted for clarity. The thermal ellipsoids are scaled to the 50% probability level.

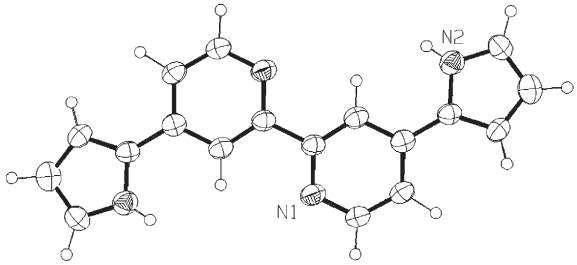

Figure 5. Solid-state structure of **7** with key atoms labeled. The thermal ellipsoids are scaled to the 50% probability level.

Conclusion

In summary, the first examples of metal-containing dipyrrolyl bipyridine receptors have been synthesized. The results presented indicate that a modification of the spacer group, that is, a replacement of the quinoxaline by a bipyridine moiety, generates a larger binding site which, inter alia, leads to an enhanced affinity for chloride anion and dihydrogen phosphate (by ca. 40- and 2600-fold, respectively). The use of a ruthenium(II) fluorophore in complex **1** provides a tool for the emission-based selective detection of phosphate at the μM level. In agreement with previously reported systems, we found that the anion affinity can be enhanced further by the introduction of a higher charge, with the triply charged Rh^{III} complex **2** displaying a greater affinity (by a factor of roughly two in the case of both chloride and benzoate anion) relative to the analogous Ru^{II} system. By increasing the number of DPB ligands on the metal center or by increasing the number of pyrrole functionalities present on the bipyridine complex core, the present approach could be used as the basis for the construction of yet-improved anion receptors. Optimization efforts directed along these lines are currently ongoing in our group.

Experimental Section

All reactions were conducted under dry argon unless otherwise stated. All solvents were of reagent grade quality and purchased commercially. Starting materials were purchased from Aldrich Chemicals, Frontier Scientific, and Strem Chemicals and used without further purification. 4,4′-Dibromo-2,2′-bipyridine[35] and *cis*-bis(2,2′-bipyridine)rhodium(III) trichloride trihydrate[36] were prepared as reported previously. NMR spectra were recorded on a Varian Mercury 400 instrument. The NMR spectra were referenced to solvent and the spectroscopic solvents were purchased from Cambridge Isotope Laboratories. Chemical ionization (CI) and electrospray ionization (ESI) mass spectra were recorded on a VG ZAB-2E and a VG AutoSpec apparatus, respectively. Elemental analyses were performed by Midwest Microlab, LLC, Indianapolis, IN. TLC analyses were carried out by using Sorbent Technologies silica gel (200 μm) or neutral alumina (200 μm) sheets. Column chromatography was performed on Sorbent silica gel 60 Å (40–63 μm) or neutral alumina (50–200 μm, Brockmann grade II). UV/Vis and emission spectra were recorded on a Beckman DU 640B and a Horiba Jobin Yvon Nanolog, respectively. For microcalorimetric titrations a MicroCal VP-ITC instrument was used.

4,4′-Bis(1-Boc-pyrrol-2-yl)-2,2′-bipyridine (6): A solution of potassium carbonate (4.00 g, 28.9 mmol) in water (20 mL) was added to 4,4′-dibromo-2,2′-bipyridine (1.60 g, 5.09 mmol), 1-Boc-pyrrole-2-boronic acid (2.80 g, 13.27 mmol), and tetrakistriphenylphosphanepalladium(0) (0.50 g, 0.43 mmol) in dimethoxyethane (200 mL). The resulting mixture was thoroughly degassed and stirred under reflux for 4 h. The organic solvent was removed, water (50 mL) was added, and the aqueous phase was extracted with dichloromethane (4×40 mL). The combined organic phases were dried over sodium sulfate, the solvent was removed in vacuo, and the product was purified by column chromatography over neutral alumina, using hexanes/ethyl acetate mixtures (4:1 to 1:1) as the eluent. Removal of the solvents and trituration with hexanes yielded 1.83 g (74%) of **6** as a colorless solid. M.p. 187°C (decomp); ^{1}H NMR (400 MHz, $CDCl_3$): $\delta=1.37$ (s, 18H; CH_3), 6.27 (dd, $J=3.4$ Hz, 2H; pyrrole-H), 6.41 (dd, $J=3.4$, 1.8 Hz, 2H; pyrrole-H), 7.29 (dd, $J=5.2$, 3.2 Hz, 2H; py-H), 7.44 (dd, $J=3.4$, 1.8 Hz, 2H; pyrrole-H), 8.45 (d, $J=1.2$ Hz, 2H; py-H), 8.62 ppm (dd, $J=5.2$, 1.2 Hz, 2H; py-H); ^{13}C NMR (100 MHz, $CDCl_3$): $\delta=27.52$, 84.42, 110.98, 116.26, 121.08, 123.32, 124.22, 132.41, 142.78, 148.45, 149.08, 155.29 ppm; HRMS (CI+): *m/z* calcd for $C_{28}H_{31}N_4O_4$ $[M+H]^+$: 487.2345; found: 487.2343; elemental analysis calcd (%) for $C_{28}H_{30}N_4O_4$: C 69.12, H 6.21, N 11.51; found: C 68.96, H 6.23, N 11.46.

4,4′-Bis-(1*H*-pyrrol-2-yl)-2,2′-bipyridine (7): Sodium methoxide (30% in methanol, 0.5 mL) was added to a solution of **6** (1.00 g, 2.06 mmol) in THF (50 mL), and the mixture was stirred for 1 h at room temperature. The organic solvent was reduced to 10 mL by using a rotary evaporator, water (100 mL) was added, and the pale pink precipitate was filtered off. This precipitate was washed with water (3×10 mL) and diethyl ether and then dried in vacuo to yield the product **7** as an off-white powder (0.57 g, 97%). M.p. >260°C (decomp); ^{1}H NMR (400 MHz, [D$_6$]acetone): $\delta=$ 6.28 (dd, $J=2.8$, 1.2 Hz, 2H; pyrrole-H), 6.86 (dd, $J=2.4$, 1.2 Hz, 2H; pyrrole-H), 7.05 (dd, $J=2.4$, 1.2 Hz, 2H; pyrrole-H), 7.61 (dd, $J=5.2$, 1.8 Hz, 2H; py-H), 8.58 (d, $J=5.2$ Hz, 2H; py-H), 8.66 (s, 2H; py-H), 11.11 ppm (br s, 2H; NH); ^{13}C NMR (100 MHz, [D$_6$]acetone): $\delta=109.59$, 110.88, 115.08, 118.59, 122.25, 130.08, 141.55, 150.29, 157.45 ppm; HRMS (CI+): *m/z* calcd for $C_{18}H_{15}N_4$ $[M+H]^+$: 287.1297; found: 287.1299; elemental analysis calcd (%) for $C_{18}H_{14}N_4$: C 75.50, H 4.93, N 19.57; found: C 75.20, H 5.11, N 19.27.

[4,4′-Bis(1*H*-pyrrol-2-yl)-2,2′-bipyridine]bis(2,2′-bipyridine)ruthenium(II) bis(hexafluorophosphate) dihydrate (1-[PF$_6$]$_2$·2H$_2$O): 4,4′-Bis(1*H*-pyrrol-2-yl)-2,2′-bipyridine (**7**, 100 mg, 0.34 mmol) and *cis*-bis(2,2′-bipyridine)ruthenium(II) dichloride dihydrate (176 mg, 0.34 mmol) were suspended in DMF (6 mL), and the solution heated to 120°C for 4 h. After cooling water (100 mL) and ammonium hexafluorophosphate (1 g) were added, the precipitate filtered off and purified by column chromatography over silica gel, using a 70:9:1 mixture of acetonitrile/water/sat. KNO_3. After removal of the bulk of the acetonitrile solvent from the desired fractions, the resulting concentrated mixture, containing ca. 5 mL of the residual eluent, was redissolved through the addition of acetonitrile (ca. 2 mL). The resulting solution was then diluted with 100 mL of water before being subject to precipitation with ammonium hexafluorophosphate (1 g).[37] The resulting precipitate was filtered off, washed with water (3× 10 mL), and dried in vacuo. This gave the product as a dark red powder (114 mg, 33%). UV/Vis (MeCN): λ_{max} ($\log\varepsilon$) = 244 (4.63), 288 (4.95), 343 (4.57), 464 nm (4.38); UV/Vis (DMSO): λ_{max} ($\log\varepsilon$) = 293 (4.94), 351 (4.58), 469 nm (4.33); ^{1}H NMR (500 MHz, [D$_6$]DMSO): $\delta=6.35$ (m, 2H; pyrrole-H), 7.19 (m, 2H; pyrrole-H), 7.23 (m, 2H; pyrrole-H), 7.49–7.57 (m, 6H), 7.62 (d, $J=6.1$ Hz, 2H), 7.73 (d, $J=6.1$ Hz, 2H), 7.90 (d, $J=$ 5.5 Hz, 2H), 8.13–8.18 (m, 4H), 8.82–8.86 (m, 6H), 11.88 ppm (br s, 2H); ^{13}C NMR (125 MHz, [D$_6$]DMSO): $\delta=110.78$, 111.93, 117.24, 119.98, 124.20, 124.34, 127.25, 127.77, 137.57, 140.46, 150.63, 151.15, 151.21, 156.53, 156.61, 156.68 ppm; HRMS (ESI+): *m/z* calcd for $C_{38}H_{31}N_8Ru$ $[M+H]^+$: 701.1715; found: 701.1720; elemental analysis calcd (%) for $C_{38}H_{30}F_{12}N_8P_2Ru\cdot 2H_2O$: C 44.50, H 3.34, N 10.92; found: C 44.44, H 3.17, N 10.47.

[4,4′-Bis(1*H*-pyrrol-2-yl)-2,2′-bipyridine]bis(2,2′-bipyridine)rhodium(III) tris(hexafluorophosphate) dihydrate (2-[PF$_6$]$_3$·2H$_2$O): 4,4′-Bis(1*H*-pyrrol-2-yl)-2,2′-bipyridine (**7**, 50 mg, 0.17 mmol) and *cis*-bis(2,2′-bipyridine)rhodium(III) trichloride trihydrate (100 mg, 0.17 mmol) were suspended in a mixture of ethanol (9 mL) and water (3 mL) and heated to reflux overnight. The ethanol was evaporated off using a rotary evaporator, water (100 mL) and ammonium hexafluorophosphate (1 g) were added, and the resulting precipitate was filtered off and purified by column chromatography over silica gel, using a 40:9:1 mixture of acetonitrile/water/sat. KNO_3. After removal of acetonitrile the resulting largely aqueous mixture, roughly 10 mL in volume, was redissolved by adding a minimum quantity of acetonitrile and diluted as above with water (ca. 100 mL), before being subject to precipitation through the addition of ammonium hexafluorophosphate (1 g). The resulting precipitate was filtered off, washed with water (3×10 mL), and dried in vacuo to give the salt as a yellow powder in 79% yield. UV/Vis (MeCN): λ_{max} ($\log\varepsilon$) = 207 (4.96), 242 (4.72), 305 (4.81), 318 (4.82), 396 nm (4.59); UV/Vis (DMSO): λ_{max} ($\log\varepsilon$): 312 (4.74), 321 (4.72), 396 nm (4.54); ^{1}H NMR (400 MHz, [D$_6$]DMSO): $\delta=6.44$ (m, 2H; pyrrole-H), 7.39 (m, 2H; pyrrole-H), 7.45 (m, 2H; pyrrole-H), 7.57 (d, $J=6.0$ Hz, 2H), 7.74–7.78 (m, 4H), 7.82 (m, 2H), 7.86 (d, $J=5.5$ Hz, 2H), 8.01 (d, $J=5.5$ Hz, 2H), 8.55 (dd, $J=$ 18.0 Hz, $J=7.5$ Hz, 4H), 8.94 (s, 2H), 9.03 (dd, $J=8.0$ Hz, 4H), 12.18 ppm (br s, 2H; NH); ^{13}C NMR (125 MHz, [D$_6$]DMSO): $\delta=111.79$, 114.96, 119.03, 120.97, 126.65, 126.73, 130.36, 130.42, 142.93, 142.96, 144.22, 149.92, 150.85, 154.24, 154.55, 154.68 ppm; HRMS (ESI+): *m/z* calcd for $C_{38}H_{30}N_8F_{12}P_2Rh$ $[M+2PF_6]^+$: 991.0932; found 991.0927; elemental analysis calcd (%) for $C_{38}H_{30}N_8F_{18}P_3Rh\cdot 2H_2O$: C 38.93, H 2.92, F 29.17, N 9.56; found: C 39.12, H 2.73, F 28.83, N 9.41.

X-ray structure determinations: Crystal structure analyses were measured on a Nonius Kappa CCD diffractometer by using a graphite monochromator with $Mo_{K\alpha}$ radiation ($\lambda=0.71073$ Å). The data were collected at 153 K by using an Oxford cryostream low-temperature device. Data reduction were performed with DENZO-SMN.[38] The structure was solved by direct methods with SIR97[39] and refined by full-matrix least-squares on F^2 with anisotropic displacement parameters for the non-hydrogen atoms by using SHELXL-97.[40] The data were corrected by using the Gaussian integration method.[40] Neutral atom scattering factors and values used to calculate the linear absorption coefficient are from the International Tables for X-ray Crystallography.[41]

Complex 1-[Cl][PF$_6$]·2H$_2$O·C$_2$H$_5$OH: Crystals grew as thin orange plates by slow evaporation from ethanol and methanol. The data crystal was a thin, square plate that had approximate dimensions 0.17×0.15×0.04 mm: triclinic, space group $P\bar{1}$, $a=12.3474(7)$, $b=13.3443(7)$, $c=13.9268(9)$ Å, $\alpha=73.891(2)$, $\beta=67.332(3)$, $\gamma=74.220(3)°$, $V=1998.7(2)$ Å^3, $Z=2$, $\rho_{calcd}=$ 1.599 g cm^{-1}, $\mu=0.578$ mm^{-1}, $F(000)=980$. A total of 241 frames of data were collected by using ω-scans with a scan range of 2° and a counting time of 310 s per frame. The structure was solved by direct methods with SIR97[39] and refined by full-matrix least-squares on F^2 with anisotropic displacement parameters for the non-hydrogen atoms by using SHELXL-97.[40] The hydrogen atoms were calculated in ideal positions with isotropic displacement parameters set to $1.2\times U_{eq}$ of the attached atom ($1.5\times U_{eq}$

for methyl hydrogen atoms). The hydrogen atoms on the two water molecules could not be reliably located in a ΔF map and were not included in the final refinement model. The function $\Sigma w(|F_o|^2-|F_c|^2)^2$ was minimized, in which $w=1/[(\sigma(F_o))^2+(0.04P)^2]$ and $P=(|F_o|^2+2|F_c|^2)/3$. The data were checked for secondary extinction effects, but no correction was necessary.

Complex 2-[Cl][PF_6]$_2$·0.5H_2O: Crystals grew as yellow lathes by slow evaporation from acetone and ethanol. The data crystal was cut from a long yellow needle and had approximate dimensions $0.33\times0.10\times0.10$ mm: orthorhombic, space group *Pbcn*, $a=40.4949(5)$, $b=8.7618(2)$, $c=23.3090(3)$ Å, $\alpha=\beta=\gamma=90°$, $V=8270.2(2)$ Å^3, $Z=8$, $\rho_{calcd}=1.664\,g\,cm^{-1}$, $\mu=0.652\,mm^{-1}$, $F(000)=4152$. A total of 561 frames of data were collected using ω-scans with a scan range of 0.5° and a counting time of 105 s per frame. The structure was solved by direct methods with SIR97[39] and refined by full-matrix least-squares on F^2 with anisotropic displacement parameters for the non-hydrogen atoms by using SHELXL-97.[40] The hydrogen atoms on carbon were calculated in ideal positions with isotropic displacement parameters set to $1.2\times U_{eq}$ of the attached atom ($1.5\times U_{eq}$ for methyl hydrogen atoms). The hydrogen atoms on the pyrrole nitrogen atoms, N3 and N4, were observed in a ΔF map and refined with isotropic displacement parameters. Two peaks in the ΔF map persisted in the vicinity of the hexafluorophosphate anions. It was reasonable to assume that these peaks might be due to some partial water molecules. The site occupancy factors were estimated to be 0.25. No hydrogen atoms for these water molecules were included in the refinement model. The function $\Sigma w(|F_o|^2-|F_c|^2)^2$ was minimized, in which $w=1/[(\sigma(F_o))^2+(0.0451P)^2+(20.6543P)]$ and $P=(|F_o|^2+2|F_c|^2)/3$. The data were checked for secondary extinction effects but no correction was necessary.

Compound 7 ($C_8H_{14}N_4$): Crystals grew as colorless needles by vapor diffusion of hexanes into a solution of the molecule in acetone. The data crystal was cut from a long needle and had approximate dimensions $0.70\times0.06\times0.05$ mm: monoclinic, space group $P2_1/n$, $a=7.763(2)$, $b=5.0730(10)$, $c=17.785(4)$ Å, $\alpha=90$, $\beta=91.514(10)$, $\gamma=90°$, $V=700.2(3)$ Å^3, $Z=2$, $\rho_{calcd}=1.358\,g\,cm^{-1}$, $\mu=0.084\,mm^{-1}$, $F(000)=300$. A total of 659 frames of data were collected using ω-scans with a scan range of 0.7° and a counting time of 89 s per frame. The structure was solved by direct methods with SIR97[39] and refined by full-matrix least-squares on F^2 with anisotropic displacement parameters for the non-hydrogen atoms by using SHELXL-97.[40] The hydrogen atoms were observed in a ΔF map and refined with isotropic displacement parameters. The function $\Sigma w(|F_o|^2-|F_c|^2)^2$ was minimized, in which $w=1/[(\sigma(F_o))^2+(0.044\,P)^2]$ and $P=(|F_o|^2+2|F_c|^2)/3$. The data were checked for secondary extinction effects. The correction took the form: $F_{corr}=kF_c/[1+(1.9(7)\times10^{-5})F_c^2\lambda^3/(\sin2\theta)]^{0.25}$ in which k is the overall scale factor.

CCDC-624410–CCDC-624412 contain the supplementary crystallographic data for this paper. These data can be obtained free of charge from The Cambridge Crystallographic Data Centre via www.ccdc.cam.ac.uk/data_request/cif.

Acknowledgements

This work was supported by the National Institutes of Health (grant GM 58907 to J. L.S.). Postdoctoral support for P.P. was provided in part by the Deutsche Forschungsgemeinschaft (DFG). P.P. would like to thank Dr. G. D. Pantos for helpful discussions.

[1] F. P. Schmidtchen, *Top. Curr. Chem.* **2005**, *255*, 1.
[2] I. Stibor, P. Zlatuskova, *Top. Curr. Chem.* **2005**, *255*, 31.
[3] P. Lhotak, *Top. Curr. Chem.* **2005**, *255*, 65.
[4] F. Davis, F. D. Collyer, S. P. J. Higson, *Top. Curr. Chem.* **2005**, *255*, 97.
[5] P. D. Beer, S. R. Bayly, *Top. Curr. Chem.* **2005**, *255*, 125.
[6] C. Suksai, T. Tuntulani, *Top. Curr. Chem.* **2005**, *255*, 163.
[7] R. J. T. Houk, S. L. Tobey, E. V. Anslyn, *Top. Curr. Chem.* **2005**, *255*, 199.
[8] *Coord. Chem. Rev.* **2003**, *240*, whole volume.
[9] J. L. Sessler, P. A. Gale, W. S. Cho, in *Anion Receptor Chemistry (Monographs in Supramolecular Chemistry)* (Ed.: J. F. Stoddart), RSC, Cambridge, **2006**.
[10] *Supramolecular Chemistry of Anions* (Eds.: A. Bianchi, K. Bowman-James, E. Garcia-Espana), Wiley-VCH, Weinheim (Germany), **1997**.
[11] *Functional Synthetic Receptors* (Eds.: T. Schrader, A. Hamilton), Wiley-VCH, Weinheim (Germany), **2005**.
[12] *Fundamentals and Applications of Anion Separations* (Eds.: B. A. Moyer, R. P. Singh), Kluwer Academic/Plenum, New York, **2004**.
[13] T. Jentsch, *Curr. Opin. Neurobiol.* **1996**, *6*, 303.
[14] J. M. Tomich, D. Wallace, K. Henderson, K. E. Mitchell, G. Radke, T. Brandt, C. A. Ambler, A. J. Scott, J. Grantham, L. Sullivan, T. Iwamoto, *Biophys. J.* **1998**, *74*, 356.
[15] D. Wallace, J. M. Tomich, , T. Iwamoto, K. Henderson, J. J. Grantham, L. P. Sullivan, *Am. J. Physiol.* **1997**, *272*, C1672.
[16] *The Biochemistry of the Nucleic Acids*, 10th ed. (Eds.: R. L. P. Adams, J. T. Knowler, D. P. Leader), Chapman and Hall, New York, **1986**.
[17] P. D. Beer, P. A. Gale, *Angew. Chem.* **2001**, *113*, 502; *Angew. Chem. Int. Ed.* **2001**, *40*, 486.
[18] W. S. Cho, J. L. Sessler, in *Functional Synthetic Receptors* (Eds.: T. Schrader, A. Hamilton), Wiley-VCH, Weinheim (Germany), **2005**, pp. 165–256.
[19] I. E. D. Vega, P. A. Gale, M. E. Light, S. J. Loeb, *Chem. Commun.* **2005**, 4913.
[20] C. B. Black, B. Andrioletti, A. C. Try, C. Ruiperez, J. L. Sessler, *J. Am. Chem. Soc.* **1999**, *121*, 10438.
[21] J. L. Sessler, H. Maeda, T. Mizuno, V. M. Lynch, H. Furuta, *Chem. Commun.* **2002**, 862.
[22] P. Anzenbacher, Jr., D. S. Tyson, K. Jursikova, F. N. Castellano, *J. Am. Chem. Soc.* **2002**, *124*, 6232.
[23] J. L. Sessler, H. Maeda, T. Mizuno, V. M. Lynch, H. Furuta, *J. Am. Chem. Soc.* **2002**, *124*, 13474.
[24] T. Mizuno, W.-H. Wei, L. R. Eller, J. L. Sessler, *J. Am. Chem. Soc.* **2002**, *124*, 1134.
[25] A larger shift is observed for the NH protons; however, in some cases the signals disappear over the course of a titration.
[26] a) C. S. Wilcox, in *Frontiers in Supramolecular Organic Chemistry and Photochemistry* (Eds.: H.-J. Schneider, H. Dürr), VCH, Weinheim (Germany), **1991**; b) K. A. Connors, *Binding Constants*, Wiley, New York, **1987**.
[27] P. D. Beer, F. Szernes, V. Balzani, C. M. Sala, M. G. B. Drew, S. M. Dent, M. Maestri, *J. Am. Chem. Soc.* **1997**, *119*, 11864.
[28] V. Amendola, M. Bonizzoni, D. Esteban-Gomez, L. Fabbrizzi, M. Licchelli, F. Sancenon, A. Taglietti, *Coord. Chem. Rev.* **2006**, *250*, 1451–1470.
[29] V. Amendola, D. Esteban-Gomez, L. Fabbrizzi, M. Licchelli, *Acc. Chem. Res.* **2006**, *39*, 343–353.
[30] T. Gunnlaugsson, P. E. Kruger, P. Jensen, J. Tierney, H. D. P. Ali, G. M. Hussey, *J. Org. Chem.* **2005**, *70*, 10875–10878.
[31] S. Camiolo, P. A. Gale, M. B. Hursthouse, M. E. Light, A. J. Shi, *Chem. Commun.* **2002**, 758–769.
[32] J. L. Sessler, D. E. Gross, W.-S. Cho, V. M. Lynch, F. P. Schmidtchen, G. W. Bates, M. E. Light, P. A. Gale, *J. Am. Chem. Soc.* **2006**, *128*, 12281–12288.
[33] M. Berger, F. P. Schmidtchen, *J. Am. Chem. Soc.* **1999**, *121*, 9986–9993.
[34] W. E. Noland, K. P. Cole, D. Britton, *Acta Crystallogr. Sect. C* **2003**, *C59*, o263-o267.
[35] G. Maerker, F. H. Case, *J. Am. Chem. Soc.* **1958**, *80*, 2745.
[36] R. D. Gillard, J. A. Osborn, G. Wilkinson, *J. Chem. Soc.* **1965**, 1951.
[37] Immediate addition of water to the aqueous slurry was avoided because it leads to the formation of difficult-to-manipulate clumps.
[38] Z. Otwinowski, W. Minor, *Methods in Enzymology: Macromolecular Crystallography, Part A* (Eds.: C. W. Carter, Jr., R. M. Sweets), Academic Press, New York, **1997**, *276*, 307–326.

[39] A. Altomare , M. C. Burla, M. Camalli, G. L. Cascarano, C. Giacovazzo, A. Guagliardi, A. G. G. Moliterni, G. Polidori, R. Spagna, *J. Appl. Crystallogr.* **1999**, *32*, 115–119.

[40] G. M. Sheldrick, SHELXL97, Program for the Refinement of Crystal Structures, University of Goettingen, Germany, **1994**.

[41] *International Tables for X-ray Crystallography, Vol. C* (Ed.: A. J. C. Wilson), Kluwer Academic, Boston, **1992**, Tables 4.2.6.8 and 6.1.1.4.

Received: October 25, 2006
Published online: January 10, 2007

